13th World Conference on Earthquake Engineering
Vancouver, B.C., Canada
August 1-6, 2004
Paper No. 2022

TORSIONAL RESPONSE OF BASE-ISOLATED STRUCTURES DUE TO STIFFNESS ASSIMETRIES OF THE ISOLATION SYSTEM

Arturo TENA-COLUNGA[1] and Christian ZAMBRANA-ROJAS[2]

SUMMARY

The torsional response of base-isolated structures when eccentricities are set in the isolation system is presented. Nonlinear dynamic analyses were used to study peak responses for different ratios of the static eccentricities between the center of mass and the center of rigidity at the isolation system (e_b), due to asymmetries in the stiffnesses of the isolators. Unidirectional and bidirectional actions of selected ground motions typical of firm soils of the Mexican Pacific Coast were used in the study. An effective period range between 1.5 and 3.0 seconds ($1.5 \text{ s} \leq T_I \leq 3.0 \text{ s}$) for the base-isolated structures was considered in the present study. Bilinear isolator systems with yield forces of 5% the weight of the complete structure ($V_y/W=0.05$) and a postyield stiffness of 10% their elastic stiffness ($k_2/k_1=0.10$) were considered. Peak dynamic responses such as maximum isolator displacements and peak displacement ductility demands were studied and compared to the ones obtained for symmetric systems of reference for the different ground motions under consideration, assessing the importance of the relative value of e_b on those response quantities. Among other relevant issues, it may be concluded from the study that eccentricities in the isolation system lead to a torsional response that adversely affects the design of the isolation system. In general, the amplification factors for the maximum isolator displacement of the asymmetric system with respect to the symmetric system increase as the eccentricity increases.

INTRODUCTION

As consequence of an extensive experimental and analytical research worldwide, particularly in New Zealand, the United States and Japan, base isolation technology is nowadays an option in seismic zones to reduce the vulnerability of structures subjected to earthquakes. There are many structural aspects that have been extensively studied regarding base isolation that have allowed the evolution of this novel technology. However, among the aspects that have received less attention is the torsional response. There are just few works available in the literature where the torsional response of base-isolated structures has been studied [1-10]. A previous work [10] summarizes the most relevant findings on the torsional response of base-isolated structures of previous studies conducted by other researchers [1, 3-8]. This section will concentrate on the findings of previous studies where the torsional response of base-isolated structures due to asymmetries in the isolation system was assessed [1-6, 8].

[1] Professor, Universidad Autónoma Metropolitana, México DF, México, e-mail: atc@correo.azc.uam.mx
[2] Graduate Student, University of California at Berkeley, USA, e-mail: zarcnek@newton.berkeley.edu

Lee [1] studied the effectiveness of bilinear hysteretic isolation systems in lowering the shear forces and torques generated in single-story structures having asymmetries in both horizontal directions subjected to the bidirectional ground motions of the 1940 El Centro record. The fixed-based periods considered for the superstructure varied from 0.1s to 1.2s, whereas the considered superstructure eccentricities were e_s/L=0, 0.1 and 0.2, and the isolation system eccentricities were e_b/L=0, 0.025, 0.05, 0.1 and 0.2. He observed the following with respect to the effect of asymmetries in the isolation system: (1) structural torques decrease as the isolation system eccentricity decrease and, (2) if the eccentricity of the isolation system is close to zero, the displacements of the base due to its rotation remain small even if the eccentricity of the superstructure is large.

Eisenberger and Rutenberg [2] investigated the effects of alternative designs of bilinear isolation systems on the seismic response of two, five and ten-story shear buildings, with one axis of symmetry and three parallel frames. The fixed based periods for these buildings were 0.25s, 0.4s and 0.8s respectively, whereas their corresponding base-isolated periods using lead-rubber bearings were 0.8s, 0.95s and 1.15s respectively. The following acceleration records of firm soils were used: (a) 1940 El Centro, (b) 1952 Taft and, (c)1977 Bucharest. Regarding the effects of eccentricities in the isolation system, they concluded that a good strategy to avoid torsional effects is designing the center of rigidity as well as the yield force center of the base isolation system to coincide with the mass axis of the superstructure, as torsional moments can effectively be eliminated for the whole range of eccentricities likely to be encountered in practice (up to 1/6 of the width).

Nagarajaiah *et al.* [3] studied torsion in multi-story base-isolated structures with inelastic elastomeric isolation systems due to bidirectional lateral ground motions of the 1940 El Centro and 1952 Taft earthquakes. They investigated the influence of various system parameters on the lateral torsional response of such systems, including the eccentricity of the isolation system. In their study, they considered the following parameters: (a) superstructure fundamental period T_s=0.5s, (b) base-isolated period T_b=2.12s, (c) superstructure frequency ratio $\Omega_{\theta s}$ =0.8, 1.0, 1.7, (d) base frequency ratio $\Omega_{\theta b}$ =0.8, 1.0, 1.7, (e) plan aspect ratio L/b=4 and, (e) uniaxial isolation eccentricity e_b/L=0, 0.065 and 0.13. They concluded the following regarding eccentricities in the isolation system: (a) the main source of torsional motions in elastomeric isolated structures is the isolation system eccentricity, (b) increasing isolation eccentricity leads to increased torque amplification, (c) an accidental isolation eccentricity of five percent may result in significant torque amplification and, (d) increasing isolation eccentricity with decreasing superstructure and base frequency ratios ($\Omega_{\theta s}$ and $\Omega_{\theta b}$) generally leads to increased corner-displacement magnifications.

Nagarajaiah *et al.* [4] also studied torsion in base-isolated structures with sliding isolation systems due to bidirectional lateral ground motions of the 1940 El Centro and 1985 Michoacán (SCT records) earthquakes. The objective of this study was to identify the key parameters that influence the torsional coupling in such systems, including strength eccentricities for the isolation system. In their study, they considered the following parameters: (a) superstructure fundamental period T_s=0.3s, 0.6s, 0.9s and 1.2s, (b) base-isolated period T_b=3s, (c) superstructure frequency ratio $\Omega_{\theta s}$ =0.8, 1.0, 1.7, (d) base frequency ratio $\Omega_{\theta b}$ =1.2, 1.7, 2.0, (e) plan aspect ratio L/b=1,4 and, (f) uniaxial isolation strength eccentricity e_b/L=0, 0.065 and 0.106. The most important conclusion on isolation eccentricity was to confirm that the strength eccentricity (e_b/L) in a sliding isolation system produces negligible torsional response regardless of the considered plan aspect ratio (L/b), an observation previously done by Zayas, Low and Mahin in 1987.

Jangid and Datta [5,6] studied the nonlinear response of torsionally coupled base isolated systems subjected to random ground motions. The base isolator consisted of an array of elastomeric bearing assumed to have an elasto-plastic hysteretic behavior. In their study, they considered the following parameters: (a) superstructure fundamental period T_s=1.0s, (b) superstructure frequency ratio $\Omega_{\theta s}$ =1.0, 2.0, (c) uniaxial superstructure eccentricity e_s/L=0, 0.15

and 0.30, (d) mass ratio m_b/m_s=1.5, (e) plan aspect ratio L/b=1, (f) normalized yield strength for the isolation system F_y/W=0.08 and, (g) uniaxial isolation eccentricity e_b/L=0, 0.15 and 0.30. Regarding isolation eccentricity, they concluded that the isolator eccentricity decreases the effectiveness of isolation for torsional deformation, increase the base displacements and decreases the superstructure displacement perpendicular to the direction of eccentricity to a much lesser extent.

As it can be observed, many studies were conducted on single-story structures subjected to earthquakes records typical of California. The only studies that considered multi-story buildings on elastomeric bearings are Eisenberger and Rutenberg [2] and Nagarajaiah *et al*. [3]. In addition, the referenced studies [2,3] were done for a reduced number of effective periods for the base-isolated structures (i.e., Nagarajaiah *et al*. [3] considered $T_b=T_I$=2.12s, Eisenberger and Rutenberg [2] considered $T_b=T_I$=0.8s, 0.95s and 1.15s). It is worth noting that in the literature, it is recognized that base isolation is most appropriate when the effective period of the isolated structure is in the range $1.5s\leq T_I\leq 3s$. Skinner *et al*. [11] proposed the lower limit and the upper limit is defined by different seismic guidelines [12, 13, 14] for using static design procedures and some options for dynamic design procedures. Therefore, a parametric study covering this period range is of utmost importance for the seismic design of base-isolated structures. Finally, most of the referenced studies considered unidirectional eccentricity and unidirectional action of the acceleration records.

The study presented herein is part of a comprehensive parametric research where the torsional response of a three-story rigid structure with bilinear (elastomeric) isolators when subjected to bidirectional lateral ground motions typical of subduction earthquakes of the Mexican Pacific Coast is studied when the eccentricity exists in: (a) the superstructure, (b) the isolation system and, (c) in both the superstructure and the isolation system. Both unidirectional and bi-directional eccentricities were considered. In this study, an effective period range for isolated structures $1.5s\leq T_I\leq 3s$ was selected. The study concentrates on peak responses for specific helpful design parameters for isolators, such as (1) displacement ductility demands, (2) peak displacements, (3) angle with respect to the global coordinates of the structural system where peak displacements occur, (4) amplification factors due to bidirectional seismic input (with respect to unidirectional input) and, (5) amplification factors because of bidirectional eccentricity (with respect to unidirectional eccentricity). In addition, amplifications of asymmetric systems with respect of counterpart symmetric systems of reference are also presented. Details of the described study can be consulted in Gómez-Soberón [9]. Some of the most relevant aspects of this research when the torsional response is due exclusively to eccentricities in the superstructure are summarized in Tena-Colunga and Gómez-Soberón [10]. This paper discusses the aspects when the torsional response is due exclusively to eccentricities in the isolation system.

STRUCTURAL MODEL CONSIDERED

The subject three-story building model is depicted in Fig. 1. The building is regular in elevation and symmetric with respect to two main orthogonal axes in mass and stiffness. Details on the structural model and their corresponding mode shapes are summarized elsewhere [9, 10]. The fundamental fixed-based periods in the main orthogonal directions are $T_x=T_y$= 0.187s. The ratio between the torsional and lateral frequencies for the superstructure is $\Omega_{\theta s}$=1.20. The plan aspect ratio is L/b=1.

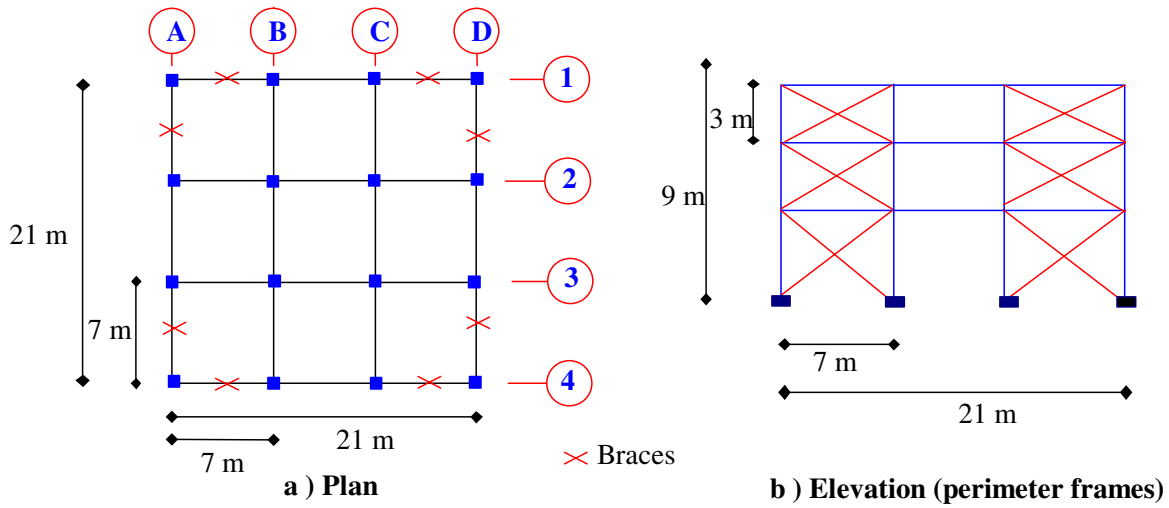

Figure 1. Model under study

CHARACTERISTICS OF THE BILINEAR ISOLATORS

In this study, bilinear isolators with a post to pre yielding stiffness of 10% (k_2/k_1=0.10) were selected (Fig. 2). The isolators were designed following some available recommendations of the New Zealand practice [11] and the 1997 Uniform Building Code (UBC-97) [12], as presented in greater details elsewhere and summarized in Tena-Colunga and Gómez-Soberón [10].

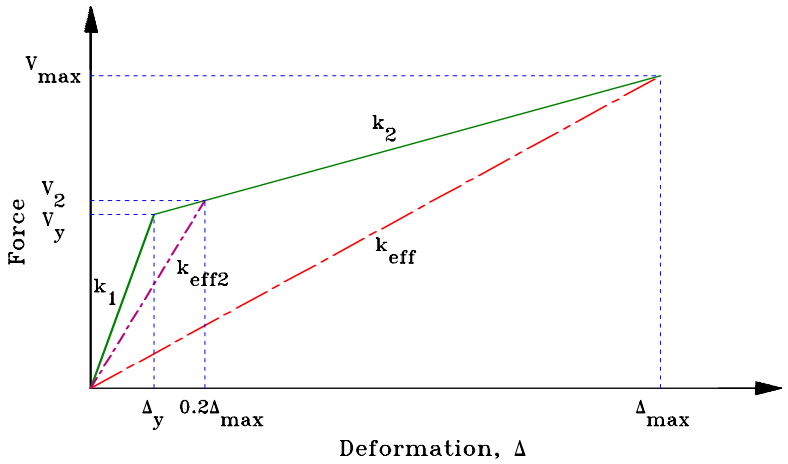

Figure 2. Design envelope curve for bilinear isolators that follow the restrictions of the UBC code.

The symmetric system of reference is depicted in Fig. 3, where all the isolators of circular cross section have an effective stiffness at the design displacement k_{1x}= k_{1y}=k_1, which are the same stiffnesses used in the study presented in Tena-Colunga and Gómez-Soberón [10] when the torsional response is due exclusively to eccentricities in the superstructure. In order to include eccentricities in the isolation system in one direction (Fig. 4) and two directions (Fig. 5), the distributions of isolators of circular cross section in plan depicted in Figs 4 and 5 were considered. In Figs. 3 to 5, k_i is the effective stiffness of the isolator type i at the design displacement in any given direction. Also, in order to provide the static eccentricities in the isolation system, $k_3 > k_1 > k_2$. It is worth noting that, in order to compare results for the different models under study, all corner isolators have the same effective stiffness at the design displacement k_1 for all models (Figs 3 to 5).

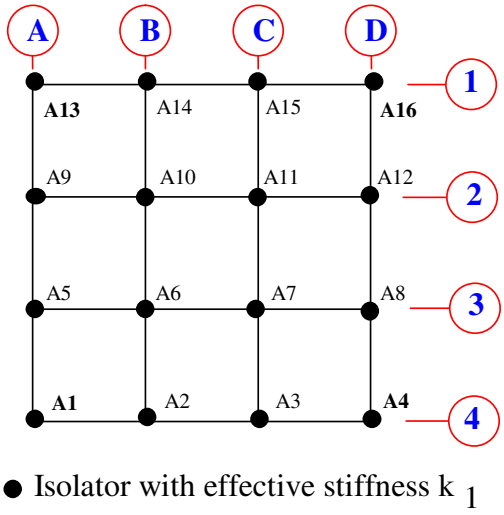

Figure 3. Symmetric isolation system of reference

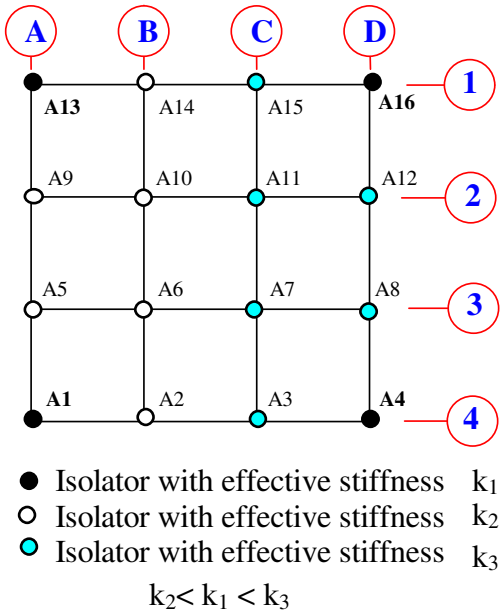

Figure 4. Stiffness eccentricity in the isolation system in one direction

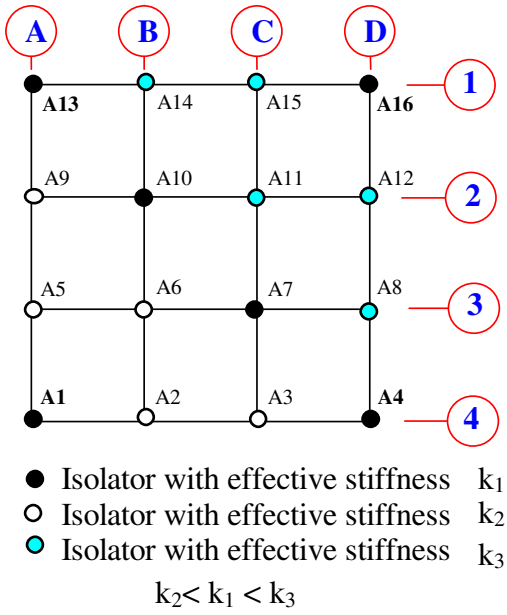

Figure 5. Stiffness eccentricity in the isolation system in two directions

It is clear that, being all isolators of circular cross section, the values for k_1, k_2 and k_3 were obtained solving the following equations, for a given effective isolated period T_I and static eccentricities e_x and e_y for the isolation system:

$$K_x = K_y = K_{eff} = \frac{4\pi^2 W}{g T_I^2} \tag{1}$$

$$K_x = K_y = \sum_{j=1}^{n} k_j = \sum k_1 + \sum k_2 + \sum k_3 \tag{2}$$

$$e_x = \frac{\sum_{j=1}^{n} k_j x_j}{K_y} = \frac{\sum_{j=1}^{n} k_j x_j}{\sum_{j=1}^{n} k_j} \tag{3}$$

$$e_y = \frac{\sum_{j=1}^{n} k_j y_j}{K_x} = \frac{\sum_{j=1}^{n} k_j y_j}{\sum_{j=1}^{n} k_j} \tag{4}$$

where W is the weight of the structure mounted on the isolation system, g is the constant of gravity, K_x is the effective lateral stiffness of the isolation system at the design displacement in the X direction, K_y is the effective lateral stiffness of the isolation system at the design displacement in the Y direction, k_j is the effective stiffness at the design displacement for isolator j, n is the total number of isolators, x_j and y_j are respectively the X and Y distances for isolator j with respect to the center of mass of the isolation system, and e_x and e_y are the static eccentricities (at the design displacement) in the X and Y directions respectively between the center of mass and the center of stiffness of the isolation system. Therefore, the definition of the static eccentricities in the isolation system (e_b) considered in this study is depicted in Figure 6.

SELECTED ACCELERATION RECORDS

As described in Tena-Colunga and Gómez-Soberón [10], a set of accelerograms typical of strong subduction earthquakes recorded in firm soil sites or rock during the past two decades in the Mexican Pacific Coast were used in the present study. The two horizontal components of the following records were considered: (a) La Unión station (**UNION**), recorded during the September 19, 1985 Michoacán earthquake (M_s=8.1), (b) San Marcos station (**SMRZA**), epicentral records for the April 25, 1989 earthquake (M_s=6.9) and, (c) Termoeléctrica station (T**MANZ**), accelerograms with site effects recorded during the October 9, 1995 Manzanillo earthquake (M_w=8.0). Some characteristics of the records are summarized in Table 1.

Table 1. Some characteristics of the selected earthquake records2

Station	Duration (s)	E-W Record		N-S Record	
		A_{max} (cm/s^2)	V_{max} (cm/s)	A_{max} (cm/s^2)	V_{max} (cm/s)
UNION	62.3	127	12.6	174	21.0
SMRZA	30.4	148	16.7	165	17.7
TMANZ	154.6	387	30.7	381	28.9

GENERALITIES OF THE PARAMETRIC STUDIES

In order to study the influence of static torsional eccentricities e_b (Fig. 6) on the dynamic response of base-isolated structures, the following range was selected for the effective period of isolated structures (T_I): 1.5s≤T_I≤3s. The lower limit (T_I=1.5s) is taken from the recommendations available in Skinner *et al.* [11] and the upper limit (T_I=3s) is taken from the UBC code [12], as this value is the limiting period set by the code for using static design procedures and some options for dynamic design procedures. Nonlinear dynamic responses of base-isolated models were computed in the selected effective period range with an effective period increment of 0.1 second, this is, there were 16 models in the period range 1.5s ≤T_I≤3s. A yield strength ratio V_y/W=0.05 for the isolation system was considered, where W=991 Ton is the total weight for the structure above the isolation system.

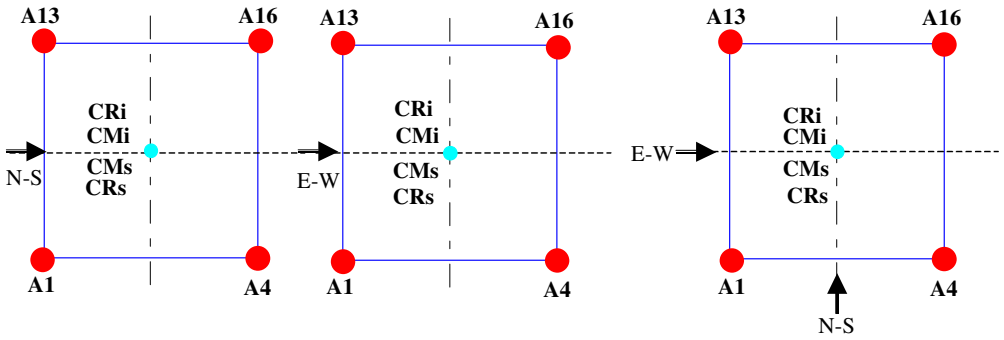

a) Symmetric system of reference (unidirectional and bidirectional input)

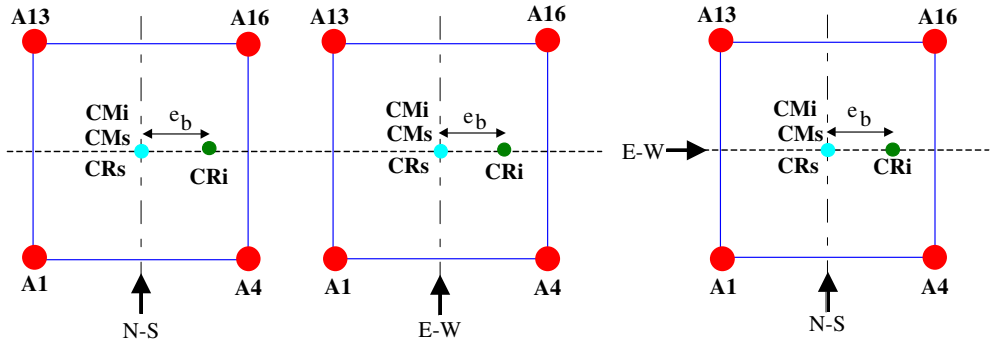

b) Stiffness eccentricity in one direction (unidirectional and bidirectional input)

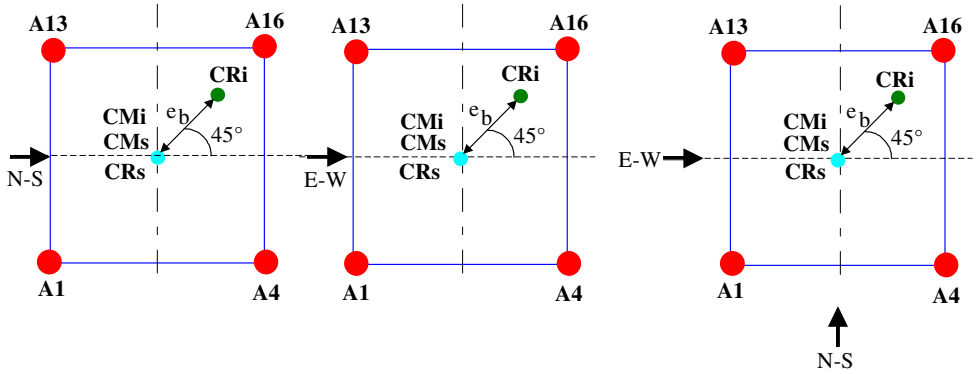

c) Stiffness eccentricity in two directions (unidirectional and bidirectional input)

Figure 6. Definition of the static eccentricities in the isolation system, e $_b$

Thus, 16 sets of data were computed for a considered yield strength, static eccentricity and action of the ground motions (unidirectional or bidirectional). For a given combination of yield strength and static eccentricity, three different actions were considered: unidirectional E-W, unidirectional N-S and bidirectional. Static eccentricities in the isolation system of 5%, 10%, 15% and 20% the floor plan dimension (L=21m) were selected, for both one direction and acting on a 45% angle, as depicted in Figures 4, 5 and 6, plus the completely symmetric case (e_b=0%, Figs. 3 and 6).

Therefore, in order to study the influence of the static eccentricity in the isolation system (e_b) in the torsional response of base isolators, a total of 1,296 simulations were needed for the set of ground motion records considered. The 3D-Basis software [15] was used for this purpose.

From the existing 16 isolators, four were selected to monitor the nonlinear response. These isolators are corner isolators A1, A4, A13 and A16 depicted in Figures 3 to 6, where it can be observed that, for all models, these corner isolators have the same effective stiffness k_1 at the design displacement. Isolators A4 and A13 were selected as they are located on intermediate distances when bidirectional eccentricity is considered (Fig. 6c) instead of concentrating on the isolator that have the shortest (A16) and largest (A1) distance from CMs, that have the smallest and higher demands, as previously done in other studies. However, when the static eccentricity e_b is in one direction, these isolators are indeed nearest (A13) and/or farthest (A4) placed from the corresponding CMs (Fig. 6b). For the completely symmetric systems (e_b=0%, Fig 6a), all isolators experience the same peak responses, as the selected ground motions induce no torsional response.

SYSTEMS WITH ECCENTRICITIES IN THE ISOLATION SYSTEM

As stated earlier, the models of reference were studied for static eccentricities e_b of 5%, 10%, 15% and 20% of the plan dimension (L=21m), for both one direction and acting on a 45% angle, as depicted in Figure 6. For illustration purposes, some results for static eccentricities of 5% and 20% will be first presented and discussed. In addition, the results obtained for bidirectional and unidirectional eccentricity will be directly compared in following sections for all the considered static eccentricities under study.

The displacement ductility demands μ obtained when the static eccentricity e_b=5% is unidirectional (Fig. 6b) when subjected to bidirectional input of the ground motions under study are depicted in Figure 7 for all corner isolators. It is observed that peak responses are obtained for TMANZ records whereas the smaller demands are associated to station SMRZA. The torsional coupling and the bidirectional input of the ground motions cause that the ductility demands for all corner isolators differ in peak values, although the ductility demand curves for isolators A1, A13, A4 and A16 are similar. Peak ductility demands are associated to isolator A1 for all the ground motion records under study, and are within the 1.5s to 2s period range approximately. In any case the peak ductility demands surpass the maximum value μ=9 associated to the primary curve recommended by the UBC provisions (Fig. 2) for the isolators under study. It is worth noting that, as expected, for unidirectional eccentricity, peak displacements for isolators A1 and A13 are almost identical, and the same happens for isolators A4 and A16.

The displacement ductility demands μ obtained when the static eccentricity e_b=5% is bidirectional (Fig. 6c) when subject to bidirectional input of the ground motions under study is depicted in Figure 8 for all corner isolators. It is also observed that peak responses are obtained for TMANZ records whereas the smallest demands are associated to station SMRZA. Peak ductility demands do not surpass the maximum value μ=9 associated to the primary UBC curve. As expected (Fig. 6c), highest demands are obtained for isolator A1 and smallest demands are obtained for isolator A16. According to Fig. 6c, and taking as a reference the CRi, for bidirectional eccentricity isolator A4 and A13 are located in the flexible side with respect to one ground motion component (A4 with E-W, A13 with N-S) and on the stiff side with the corresponding orthogonal component (A4 with N-S, A13 with E-W), so in this case, it is not clear, *a-priori*, which isolator will experience higher demands. As discussed in a previous work [10], this is an important difference of this research with respect to other studies that have just concentrated on the isolators subjected to smallest (A16) and highest (A1) demands, but give no insight on what may happen in isolators that may be placed somewhat in between (A4 and A13).

It is observed in Figure 8 that for all stations, isolator A13 is almost always subjected to higher ductility demands than isolator A4 over all the considered period range, except for the period range between 1.8s and 2.2s under TMANZ and between 2.7s and 3.0s under UNION.

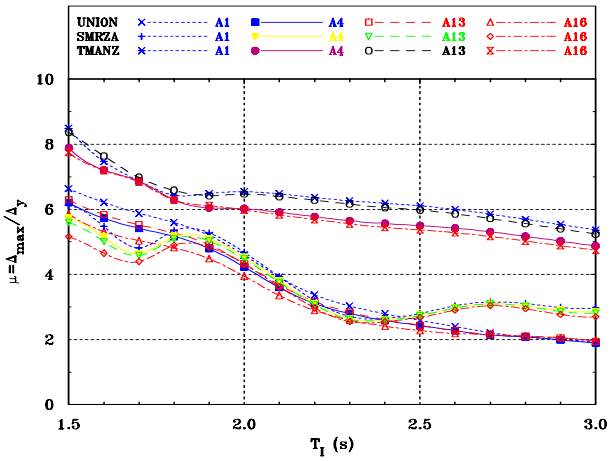

Figure 7. Ductility demands (μ) for corner isolators when e_b=5% is unidirectional and under bidirectional seismic input.

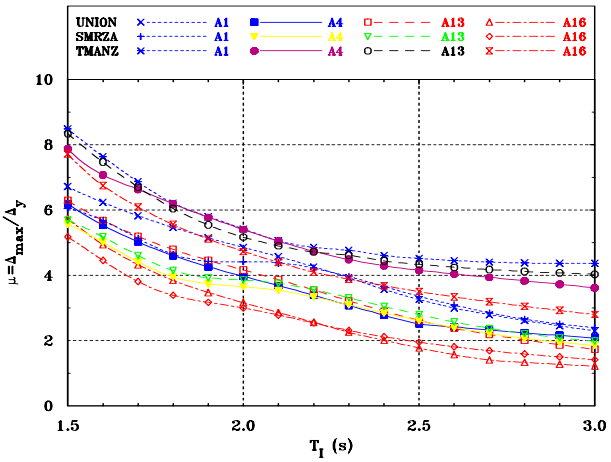

Figure 8. Ductility demands (μ) for corner isolators when e_b=5% is bidirectional and under bidirectional seismic input.

If the results plotted in Figure 7 for TMANZ are compared with those of Figure 8, one can observe that in general, torsional coupling under bidirectional eccentricity decreases the ductilty demands of all corner isolators with respect to unidirectional eccentricity for the period range between 1.8s to 3.0s. For the other considered records, there are period ranges where this response is increased, but in other periods the response is decreased. These would be unexpected results if one considers that the dynamic torques resulting from the eccentricities in each given orthogonal direction always add. Nevertheless, it is clear that the resulting dynamic torques can also act in opposite directions (subtract); therefore, the provided results suggest that peak demands under bidirectional eccentricities are generally associated to time steps where the resulting dynamic torques acted in opposite directions for the pairs of acceleration records considered in this study.

The trend observed on the variation of μ for other static eccentricities (10%, 15% and 20%) are similar to those shown for e_b=5%, but associated to higher demands, so for illustration purposes only the curves for e_b=20% when V_y/W=0.05 are shown. The displacement ductility demands μ obtained under bidirectional input of the ground motions is depicted in Figure 9 when e_b is unidirectional (Fig. 6b) and in Figure 10 when e_b is bidirectional (Fig. 6c).

It is observed with respect to the results plotted in Figures 7 and 8 for e_b=5% that: (a) as the static eccentricity increases, ductility demands (μ) clearly increase for all isolators, (b) ductility demands (μ) increase faster for isolator A1 than for isolator A16 for both unidirectional and bidirectional static eccentricities, (c) there is more difference in the ductility demands (μ) for isolators A13 and A4 for unidirectional static eccentricity than for bidirectional static eccentricity, particularly for TMANZ. The curves for isolators A4 and A13 differentiate more when the static eccentricity is unidirectional, because for this case it is clear that one isolator is located on the flexible side while the other is on the stiff side, whereas this difference is smaller when the e_b is bidirectional, where no isolator is really located on a flexible or stiff side, so the amplifications depends on the characteristics of each ground motion component and its directivity as assumed in this study, (d) For TMANZ records, peak ductility demands for all corner isolators surpass the maximum value μ=9 associated to the primary curve recommended by the UBC provisions when e_b=20% is unidirectional in the period range 1.5s to 2.5s (Figure 9), and for all corner isolator except A16 in the period range 1.5s to 2.4s when e_s=20% is bidirectional (Figure 10) and, (e) As observed for e_b=5%, torsional coupling under bidirectional eccentricity (Fig. 10) decreases the

ductility demands of all corner isolators with respect to those obtained under unidirectional eccentricity (Fig. 9) for most of the considered period range under study and for all records.

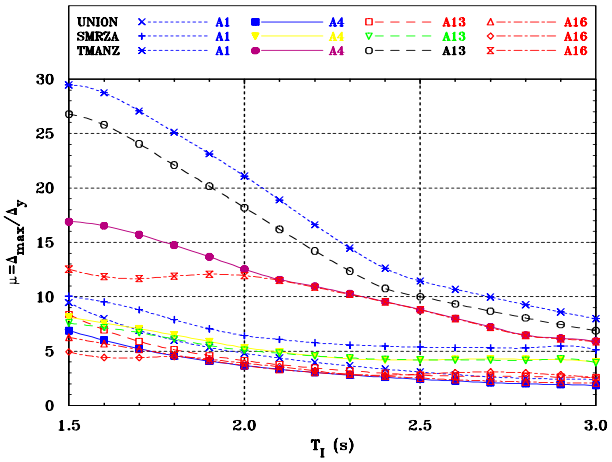

Figure 9. Ductility demands (μ) for corner isolators when e_b=20% is unidirectional and under bidirectional seismic input.

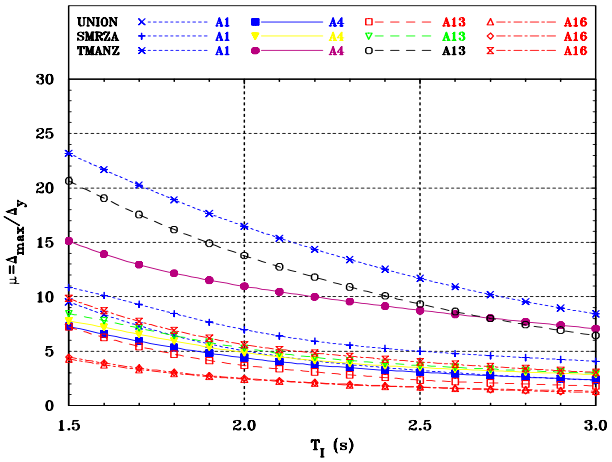

Figure 10. Ductility demands (μ) for corner isolators when e_b=20% is bidirectional and under bidirectional seismic input.

COMPARISON OF PEAK ISOLATOR DISPLACEMENTS BETWEEN UNIDIRECTIONAL OR BIDIRECTIONAL STATIC ECCENTRICITY IN THE ISOLATION SYSTEM

It is important to assess the relative difference in the peak displacement demands for the isolators when the eccentricity in the superstructure is only in one direction (Figure 6b) or in two directions (Figure 6c), when the system is subjected to bidirectional input of the ground motions under consideration.

A-priori, one would assume that peak responses would generally occur when the static eccentricity is bidirectional (Figure 6c), if one considers that the dynamic torques resulting from the eccentricities in each given orthogonal direction always add. As mentioned earlier, the resulting dynamic torques under bidirectional static eccentricity can also act in opposite directions (subtract), so the dynamic relation is more complex. This is shown in Figures 11 for SMRZA records and in Figure 12 for TMANZ records, where the relative ratio between peak isolator displacements for bidirectional eccentricities [Δ_{max}(e2D)] and unidirectional eccentricities [Δ_{max}(e1D)] for critical isolator A1 is depicted when subjected to bidirectional ground motion input. From the observation of Figures 11 and 12, and other figures obtained for V_y/W=0.05 for all the ground motion records and corner isolators considered in this study (not shown), one may conclude that Δ_{max}(e2D)/ Δ_{max}(e1D) ratio depends on many parameters, among them: (a) characteristics of the ground motions and their directivity, (b) dynamic coupling of the base isolated structure with the ground motions, (c) the relative eccentricity ratio presented in the isolation system, (d) the location of a given isolator in plan, (d) the own characteristics of the isolators. For the bilinear isolators considered in this study, it is clear that this depends on the yield strength ratio V_y/W, comparing the results for V_y/W=0.05 (shown) with those for V_y/W=0.10 (not shown). By extension, the authors assume that differences would also be observed for different pre to post yielding stiffness ratio from the one considered in this study (k_2/k_1=0.10), but this has to be confirmed with specific studies devoted to study this parameter.

It is worth noting that often, peak displacements under unidirectional eccentricity could be higher than those for bidirectional eccentricity for a given isolator, in this particular case, isolator A1 (Figures 11 and 12), as the dynamic torques under bidirectional static eccentricity acted in opposite directions, so the

resulting effective dynamic torque under bidirectional static eccentricity is smaller than the one obtained under unidirectional static eccentricity.

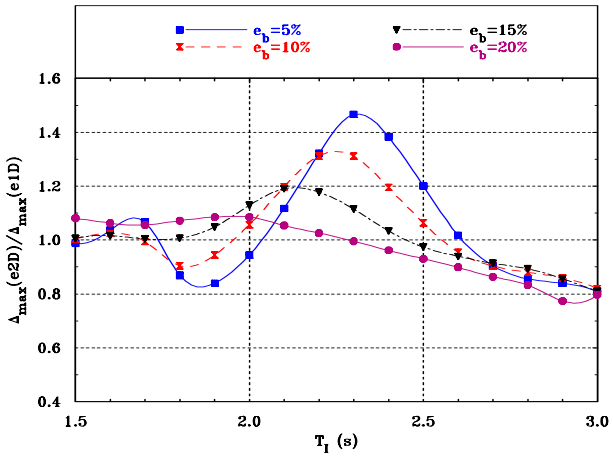

Figure 11. Relative ratio between peak isolator displacements for bidirectional and unidirectional eccentricities for critical isolator A1, SMRZA records.

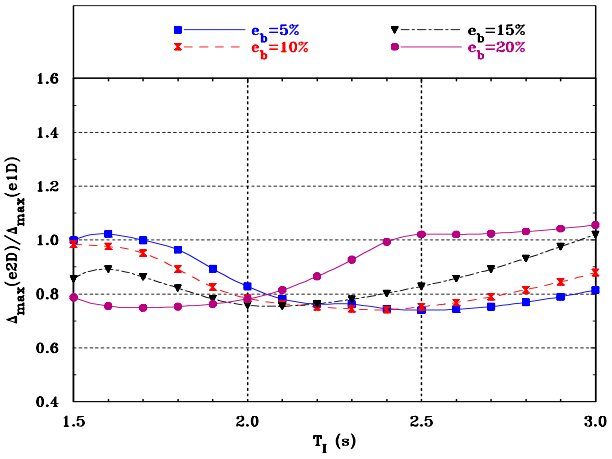

Figure 12. Relative ratio between peak isolator displacements for bidirectional and unidirectional eccentricities for critical isolator A1, TMANZ records

COMPARISON OF PEAK ISOLATOR DISPLACEMENTS FOR SYSTEMS WITH ASYMMETRIES AT THE ISOLATION LEVEL VS. SYMMETRIC SYSTEMS

In order to compare the peak displacements experienced by the corner isolators under study (A1, A4, A13 and A16) when there are no eccentricities (symmetric systems, Fig. 6a) with those when there are eccentricities in the isolation system (asymmetric systems, Figs. 6b and 6c), peak displacements for the isolators of asymmetric systems [$\Delta_{max}(e_b)$] were divided by those of symmetric systems [$\Delta_{max}(e=0)$]. Both unidirectional (Fig. 6b) and bidirectional eccentricities (Fig. 6c) were considered.

The curves obtained for unidirectional and bidirectional eccentricities are somewhat similar. Peak amplifications and deamplifications in the period range of interest varied in function of the considered ground motion. For example, for TMANZ records, peak values were generally detected for unidirectional eccentricity; in contrast, they were obtained for bidirectional eccentricity for UNION records. For SMRZA records, curves and values were similar for most isolators, but peak deamplifications were obtained for bidirectional eccentricity for isolator A16. Therefore, the results for isolators A1 and A16 are shown in Figures 13, 15 and 17, and for isolators A4 and A13 in Figures 14, 16 and 18, considering that the most interesting results are for bidirectional eccentricity for UNION (Figs. 13 and 14) and SMRZA (Figs. 15 and 16) records, and for unidirectional eccentricity for TMANZ records (Figs. 17 and 18).

It is observed from Figs. 13, 15 and 17 that for the period range under consideration, peak displacements (and hence, ductility demands) for isolator A1 are always amplified for asymmetric systems with respect to symmetric systems, particularly for TMANZ records. Peak amplification factors of 1.54, 2.18 and 4.17 are respectively observed for isolator A1 for stations UNION (T_I=1.5s, Fig. 13), SMRZA (T_I=2.3s, Fig. 15) and TMANZ (T_I=1.9s, Fig. 17) when the static eccentricity is e_b=20%.

On the other hand, peak displacements for isolator A16 are generally reduced for asymmetric systems with respect to the symmetric systems due to the torsional response, being particularly important for SMRZA

records, where it is observed that for e_b=20% and T_I=3.0s, the smallest isolator displacement is only about 0.43 times the one obtained for the symmetric system (Fig. 15).

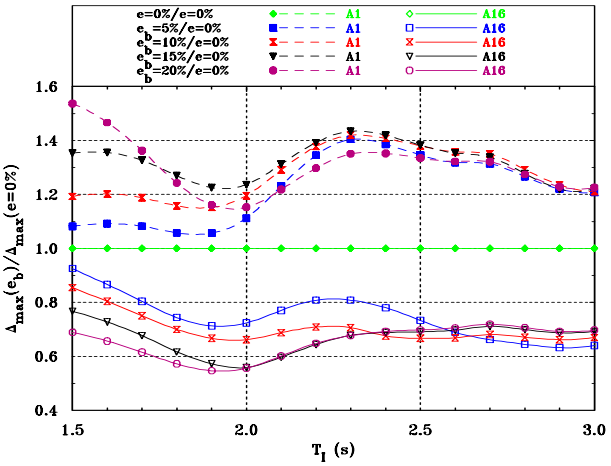

Figure 13. Ratio for peak isolator displacements of asymmetric systems with respect to symmetric systems for isolators A1 and A16 for UNION records.

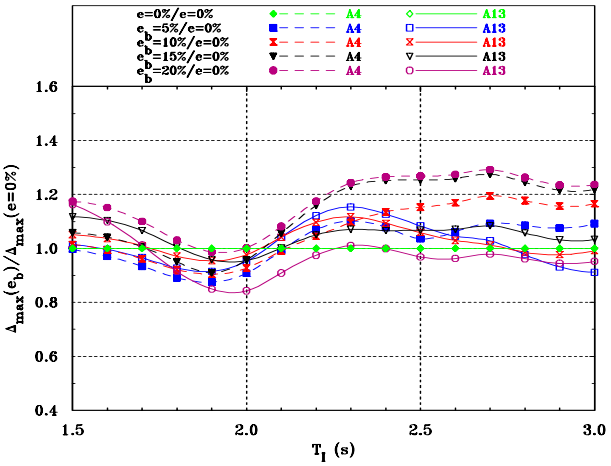

Figure 14. Ratio for peak isolator displacements of asymmetric systems with respect to symmetric systems for isolators A4 and A13 for UNION records.

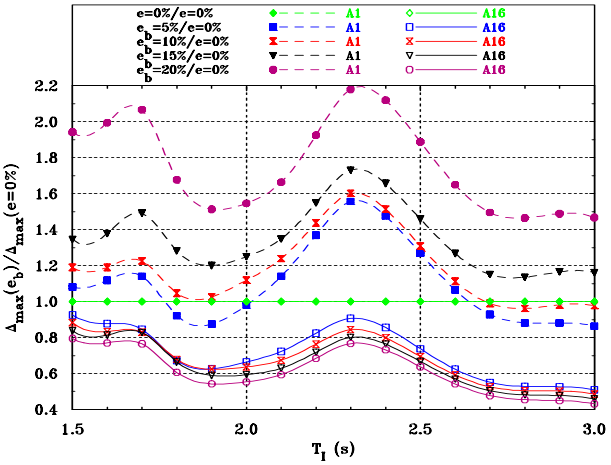

Figure 15. Ratio for peak isolator displacements of asymmetric systems with respect to symmetric systems for isolators A1 and A16 for SMRZA records.

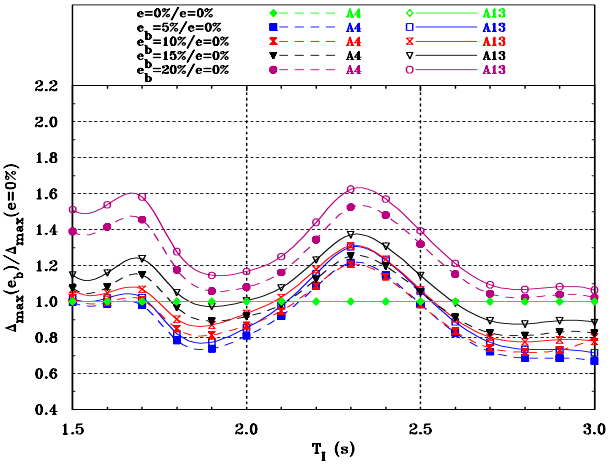

Figure 16. Ratio for peak isolator displacements of asymmetric systems with respect to symmetric systems for isolators A4 and A13 for SMRZA records.

Therefore, it is concluded that for the ground motions under consideration, extreme cases of torsional response have an important contribution on the total displacement of extreme corner isolators A1 and A16. For e_b=20%, the torsional component contributes with up to 76% of the total displacement for isolator A1 and TMANZ records, and with up to 57% of the total displacement for isolator A16 and SMRZA records.

It is observed from Figs. 14, 16 and 18 that peak displacements for isolator A4 are generally amplified for asymmetric systems with respect to symmetric systems, particularly for TMANZ records. However, for SMRZA and UNION records, there are period ranges where the displacements for asymmetric systems are usually smaller than those of symmetric systems (Figs. 14 and 16). Peak amplification factors of 1.29, 1.52

and 2.46 are respectively observed for isolator A4 for stations UNION (T_I=2.7s, Fig. 14), SMRZA (T_I=2.3s, Fig. 16) and TMANZ (T_I=1.9s, Fig. 18) when the static eccentricity is e_b=20%.

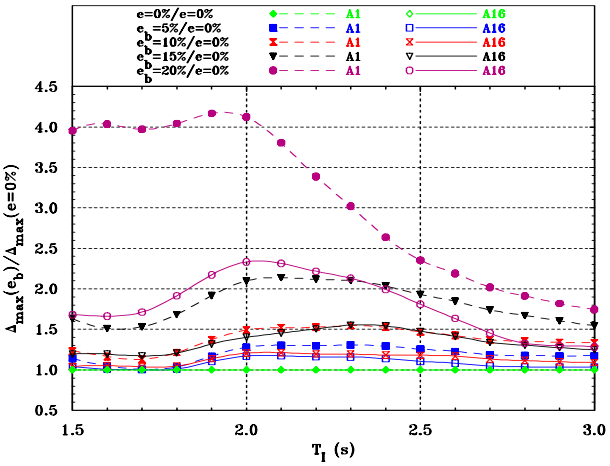

Figure 17. Ratio for peak isolator displacements of asymmetric systems with respect to symmetric systems for isolators A1 and A16 for TMANZ records.

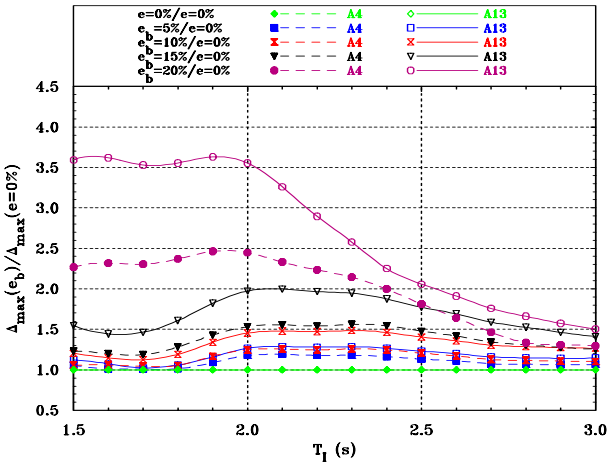

Figure 18. Ratio for peak isolator displacements of asymmetric systems with respect to symmetric systems for isolators A4 and A13 for TMANZ records.

Similar observations to the ones done for isolator A4 can be done for isolator A13 regarding amplification or deamplification of asymmetric systems with respect to symmetric systems, but peak amplifications are higher for isolator A13 than for isolator A4 for SMRZA and TMANZ records. Peak amplification factors of 1.16, 1.63 and 3.63 are respectively observed for isolator A13 for stations UNION (T_I=1.5s, Fig. 14), SMRZA (T_I=2.3s, Fig. 16) and TMANZ (T_I=1.9s, Fig. 18) when the static eccentricity is e_b=20%.

The following general observations can be done for all corner isolators under study (A1, A4, A13 and A16): (a) As expected, amplifications (or deamplifications) on the response of asymmetric systems with respect to symmetric systems increase as the static eccentricity increases, and it is particularly evident for e_b=20% for TMANZ and SMRZA records, (b) The $[\Delta_{max}(e_b)]/[\Delta_{max}(e=0\%)]$ ratio is not constant in the period range under consideration for all the selected ground motions and, (c) The characteristics of these amplification (deamplification) curves vary for each set of ground motion records in shape and the location of peak amplification or deamplification factors. Therefore, it seems that the characteristics of these curves strongly depend on the own characteristics of the selected ground motions, even though all records correspond to firm soil sites. Similar observations were made when static eccentricities were set in the superstructure [10]. The major difference in the results obtained for static eccentricities in the superstructure compared to those obtained for static eccentricities in the isolation system, is that for large eccentricities (15% and 20%), the displacement demands for the corner isolator are much higher when the eccentricity is set in the isolation system, particularly when e_b=20%.

CONCLUSIONS

Based upon the parametric study for the bilinear isolators briefly described in this paper, one can do the following observations:

With respect to the ductility demands (μ) for the corner isolators under study, one can conclude that: (a) As expected, as the static eccentricity e_b increases, ductility demands (μ) clearly increase for isolator A1 and decrease for isolator A16 for both unidirectional and bidirectional eccentricities, (b) ductility demands

(μ) clearly increase for isolator A4 and decrease for isolator A13 for unidirectional static eccentricity, both for bidirectional static eccentricity the relation is much more complex, (c) for all corner isolators, the amplification curves due to static eccentricities strongly depend on the characteristics for each ground motion component and its directivity as assumed in this study and, (d) Peak ductility demands surpass the maximum value μ=9 associated to the primary curve recommended by the UBC provisions for all isolators when the static eccentricity (unidirectional or bidirectional) is e_b >10% over a important period range, particularly for TMANZ records. This fact is illustrated in this paper for e_b=20%.

As shown in a previous study when the static eccentricities were set in the superstructure [10], peak displacements for a given isolator do not generally occur when the static eccentricity in the isolation system is bidirectional, as they may occur when the static eccentricity is unidirectional instead. The relative ratio between peak isolator displacements for bidirectional eccentricities [Δ_{max}(e2D)] and unidirectional eccentricities [Δ_{max}(e1D)] is more complex, as this ratio depends on many parameters, among them: (a) characteristics of the ground motions and their directivity, (b) dynamic coupling of the base isolated structure with the ground motions, (c) eccentricity ratio for the isolation system, (d) the location of a given isolator in plan and, (e) the own characteristics of the isolators, among some of the most identifiable parameters.

Based upon the comparative study of the peak displacements experienced by the selected isolators when there are no eccentricities (symmetric systems) with those when there are eccentricities in the isolation system (asymmetric systems), one can conclude that: (a) as expected, amplifications (or deamplifications) on the response of asymmetric systems with respect to symmetric systems increase as the static eccentricity increases, (b) the amplification (deamplification) ratio is no constant in the period range under consideration for all the selected ground motions, (c) the characteristics of these amplification (deamplification) curves vary for each set of ground motion records, both in the shape and in the location of peak amplification or deamplification factors, and (d) extreme cases of torsional response have an important contribution on the total displacement of corner isolators. The torsional component contributed with up to 76% of the total displacement for a corner isolator when the static eccentricity was e_b=20% for TMANZ records.

In general, this study agrees with the studies of Lee [1], Eisenberger and Rutenberg [2] and Nagarajaiah *et al.* [3] in concluding that the effectiveness of base isolation for torsionally coupled systems decreases with increase of the eccentricity in the isolation system, although it is worth noting that this study considered a wider period range for base-isolated structures than the former studies of reference. Also, this study tends to agree with Nagarajaiah *et al.* [3] in concluding that the main source of torsional motions in elastomeric isolated structures seems to be the isolation system eccentricity, particularly when the eccentricity is large (greater than 10%). However, this observation needs to be confirmed with more detailed studies, which must include a wider range of base frequency ratios ($\Omega_{\theta s}$ and $\Omega_{\theta b}$) than the ones used in this study and in Nagarajaiah *et al.* [3].

The authors are of the opinion that, for design purposes, it would be desirable to restrict the use of static or simplified dynamic methods of analysis for base-isolated structures in building codes based upon a specific eccentricity ratio for the isolation system, as it was previously proposed when considering eccentricities in the superstructure [10]. The target eccentricity ratio for the isolation system should be set in order to distinguish when the expected design displacements associated with a given code are not well covered when compared to nonlinear dynamic analyses. This study cannot conclude on this regard, as the effects of torsional to lateral frequency ratios ($\Omega_{\theta s}$ and $\Omega_{\theta b}$) ($\Omega_{\theta s}$) must be carefully assessed. Therefore, additional research efforts are needed in this direction.

ACKNOWLEDGEMENTS

Financial support of the National Science and Technology Council of Mexico (Conacyt) and Universidad Autónoma Metropolitana Azcapotzalco are gratefully acknowledged. Luis Gómez-Soberón also collaborated in this research project, but the results of his models were not available on time to be included in this paper.

REFERENCES

1. Lee, D M (1980), "Base isolation for torsion reduction in asymmetric structures under earthquake loading," *Earthquake Engineering and Structural Dynamics*, 8: 349-359.
2. Eisenberger, M and A Rutenberg (1986), "Seismic base isolation of asymmetric shear buildings," *Engineering Structures*, 8(1): 2-9.
3. Nagarajaiah, S, A M Reinhorn and M C Constantinou (1993), "Torsion in base isolated structures with elastomeric isolation systems," *ASCE Journal of Structural Engineering*, 119(10): 2932-2951.
4. Nagarajaiah, S, A M Reinhorn and M C Constantinou (1993), "Torsional coupling in sliding base-isolated structures," *ASCE Journal of Structural Engineering*, 119(1): 130-149.
5. Jangid, R S and T K Datta (1994), "Nonlinear response of torsionally coupled base isolated structure," *ASCE Journal of Structural Engineering*, 120(1): 1-22.
6. Jangid, R S and T K Datta (1994), "Seismic response of torsionally coupled structures with elastoplastic base isolation," *Engineering Structures*, 16(4): 256-262.
7. Tena-Colunga, A, C Gómez-Soberón and A Muñoz-Loustaunau (1997), "Seismic isolation of buildings subjected to typical subduction earthquake motions for the Mexican Pacific Coast," *Earthquake Spectra,* 13(3): 505-532.
8. Almazán, J L and J C de la Llera (2000), "Lateral torsional coupling in structures isolated with the frictional pendulum system," *Proceedings of the 12th World Conference on Earthquake Engineering*, Auckland, New Zealand, paper 1536, CD-ROM.
9. Gómez-Soberón, L A A (2000), "Efectos de torsión en estructuras aisladas sísmicamente en su base," *M.S. Thesis*, División de Estudios de Posgrado de la Facultad de Ingeniería, UNAM, September (in Spanish).
10. Tena-Colunga, A and L A Gómez-Soberón (2002), "Torsional response of base-isolated structures due to asymmetries in the superstructure," *Engineering Structures*, 24(12): 1587-1599.
11. Skinner, R I, W H Robinson and G H Mc Verry (1993), **An introduction to seismic isolation**, John Wiley and Sons, London.
12. "Uniform Building Code, 1997 Edition," (1997), International Conference of Building Officials, Whittier, California.
13. "International Building Code, 2000 Edition," (2000), International Conference of Building Officials, Whittier, California.
14. FEMA-273 (1997), "NEHRP guidelines for the seismic rehabilitation of buildings," FEMA Publication 273, Federal Emergency Management Agency, Washington, D. C., October.
15. Nagarajaiah, S, A M Reinhorn and M C Constantinou (1991), "3D-Basis: Non-linear dynamic analysis of three-dimensional base isolated structures: Part II," *Technical Report NCEER-91-0005*, National Center for Earthquake Engineering, State University of New York at Buffalo.